Biochimica et Biophysica Acta 1848 (2015) 1331–1340

Contents lists available at ScienceDirect

Biochimica et Biophysica Acta

journal homepage: www.elsevier.com/locate/bbamem

Bilirubin, model membranes and serum albumin interaction: The influence of fatty acids

Pavlína Novotná [a], Marie Urbanová [b,*]

[a] Department of Analytical Chemistry, University of Chemistry and Technology, Prague, Technická 5, 166 28 Prague 6, Czech Republic
[b] Department of Physics and Measurements, University of Chemistry and Technology, Prague, Technická 5, 166 28, Prague 6, Czech Republic

ARTICLE INFO

Article history:
Received 22 October 2014
Received in revised form 31 January 2015
Accepted 25 February 2015
Available online 4 March 2015

Keywords:
Electronic circular dichroism
Liposome
Bilirubin–lipid interaction
Bilirubin–albumin interaction
Fatty acid

ABSTRACT

Electronic circular dichroism (ECD), absorption and fluorescence spectroscopy were used to study the enantioselective interactions which involved bilirubin (BR), liposomes, human serum albumin of two different purities, pure (HSA) and non-purified of fatty acids (FA-HSA), and individual fatty acids.
The application of the ECD technique to such a complex problem provided a new perspective on the BR binding to liposomes. Our results demonstrated that in the presence of pure HSA, BR preferred to bind to the protein over the liposomes. However, in the presence of FA-HSA, BR significantly bound to the liposomes composed either of DMPC or of sphingomyelin and bound only moderately to the primary and secondary binding sites of FA-HSA even at high BR concentrations. For the DMPC liposomes, even a change of BR conformation upon binding to the primary binding site was observed. The individual saturated fatty acids influenced the BR binding to HSA and liposomes in a similar way as fatty acids from FA-HSA. The unsaturated fatty acids interacted with BR alone and prevented it from interacting with either 99-HSA or the liposomes. In the presence of arachidonic acid, BR interacted enantioselectively with the liposomes and only moderately with 99-HSA.
Hence, our results show a substantial impact of the liposomes on the BR binding to HSA. As a consequence of the existence of fatty acids in the blood plasma and in the natural structure of HSA, BR may possibly bind to the cell membranes even though it is normally bound to HSA.

1. Introduction

Every day a certain amount of "old" blood cells is replaced by newly produced ones. During this process, an orange-colored pigment bilirubin (BR) is formed as a product of the decomposition of the blood pigment heme. BR is afterwards converted to a more water-soluble form and is excluded from the body [1]. BR belongs to the group of non-planar tetrapyrrolic pigments which form a helical spatial structure, with either a P- or M-sense of helicity [2–5] (Fig. 1). The racemization barrier between these two forms is low, and because of this, the P- and M-forms interconvert rapidly. Therefore, BR exists as a racemate in a homogenous solution and also when it is unbound in the blood plasma. Although there are several polar groups in the BR structure, it behaves mostly as a nonpolar compound, because the polar groups are intramolecularly connected with hydrogen bonds [2–5].

Although it is a waste product, BR fulfills a wide range of biological activities in the human body [1]. In the pathologic state, BR may accumulate and at higher concentrations its negative effects may appear [6–17]. Among the most discussed effects of BR are its deposition in tissues and its influence on nerve cell membranes which may result in cell disturbance. Moreover, BR binding to brain nerve cells is supposed to be one of the main causes of BR encephalopathy in jaundiced newborns. The interaction of BR with cells was previously studied both for model situations and in physiological conditions [13–16,18–28]. It was found that BR preferentially interacts enantioselectively with different liposomic models of cell membranes [18–20,29]. This means that one of the two enantiomeric forms (P- or M-form) of BR binds more to the liposomes and because the two forms interconvert very rapidly, the non-bound BR remains racemic. The enantiodiscrimination of BR on the membranes is supposed to be one of the primary causes of the described neurotoxic effects of BR. Because of the chiral nature of this interaction, chiroptical techniques, electronic and vibrational circular dichroism (ECD, VCD) were advantageously used to study bound BR and its effects [18,29].

Under the normal conditions in the human body, BR should not be dangerous to our well-being because it is mainly transported in the

Abbreviations: 99-HSA, 99% pure HSA; AA, arachidonic acid; BR, bilirubin; DLS, dynamic light scattering; DMPC, 1,2-dimyristoyl-*sn*-glycero-3-phosphocholine; ECD, electronic circular dichroism; FA, fatty acid; FA-HSA, human serum albumin with 4% of fatty acids; HSA, human serum albumin; IR, infrared; LA, linoleic acid; LUV, large unilamellar vesicle; MA, myristic acid; OA, oleic acid; PA, palmitic acid; SA, stearic acid; UV–Vis, ultraviolet–visible

* Corresponding author at: Department of Physics and Measurements, Institute of Chemical Technology, Prague, Technická 5, 166 28 Prague 6, Czech Republic. Tel.: +420 220443036; fax: +420 220444334.
E-mail address: Marie.Urbanova@vscht.cz (M. Urbanová).

http://dx.doi.org/10.1016/j.bbamem.2015.02.026
0005-2736/

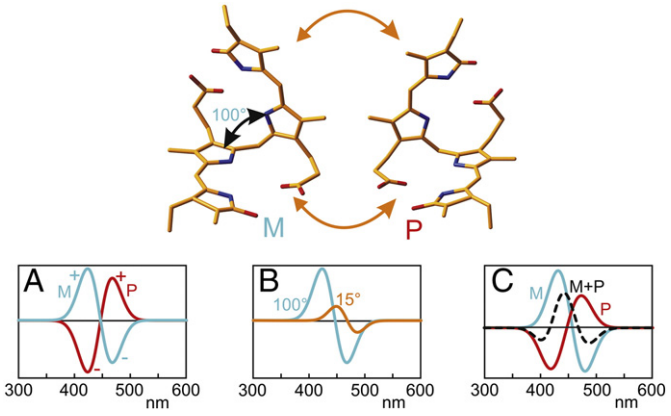

Fig. 1. Spatial structure of the M- and P-forms of BR with the dihedral angle estimated for BR in aqueous solution. (A) The negative couplet (spectral shape composed of two neighboring bands of opposite signs, negative band being at a higher wavelength than the positive) and positive couplet observed typically in the ECD spectra for the M- and P-forms of BR, respectively. (B) A simulation of the influence of the dihedral angle in the BR structure on the ECD spectra estimated with the exciton coupling method (ref. [26]), note a shift of the couplet position and the decrease of its intensity. (C) A simulated spectral overlap possible for the ECD spectra of the M- and P-forms of BR with different dihedral angles in their structure.

blood plasma by human serum albumin (HSA), one of the most abundant carrier proteins. The HSA structure is comprised of three domains, each of which consists of subdomains. The protein has extensive binding possibilities for different drugs, drug-analogs, hormones, steroids and small molecules, and also works as a main transporter of fatty acids (FAs) in the blood plasma. FAs are in fact primary ligands for HSA and at least seven different binding sites of FAs were described in the HSA structure [30–33] with very diverse binding affinities [34]. BR has three potential binding sites in the structure of HSA: one primary site located in subdomain IIA of HSA with a considerably high binding constant ($K_a \sim 10^8\ M^{-1}$) and two secondary sites located in subdomains IB and IIIA with lower and similar binding constants ($K_a \sim 10^6\ M^{-1}$) [35–39]. Remarkably, BR preferentially binds in its P-form to all three binding sites of HSA [35,36,39–43]. It should be noted here that due to the difference in the binding constants, the binding to the secondary sites occurs mostly after the primary site has been saturated. So we cannot observe the binding to the secondary sites alone unless the primary site is blocked by another compound.

Our study is aimed at the situations that may arise on the molecular level in the human body both during standard and pathologic states. As the enantioselective interaction of BR with liposomic models of membranes was confirmed [18,29], our present study focuses on the ternary systems of BR with liposomes and HSA. The object of our study is, first, whether BR will bind to the liposomes even in the presence of HSA, for which it has a high binding constant, and, second, what would occur at increased concentrations of BR when some of the HSA binding sites would be occupied by BR or by other compounds. Previous studies [44,45] showed that the tendency of BR to bind to HSA is mostly higher than to liposomes, but they proved a strong dependence on the ambient conditions and liposome composition.

Hence, we studied the influence of HSA on the BR interactions with liposomes composed of 1,2-dimyristoyl-*sn*-glycero-3-phosphocholine (DMPC, a model of ordinary cells) and of sphingomyelin (a model of nerve cells). These two types of liposomes were chosen, because they serve as an appropriate model of natural membranes [29]. Our previous study [29] also showed a negligible effect of cholesterol on the interactions of the selected liposomes with BR and, therefore, cholesterol was not included in this study. Only a few tests were run for each studied system to confirm that its presence did not influence the systems with the FAs and serum albumins used.

As it is mainly unbound free BR, the effects of which are neurotoxic, and because its concentration is strongly influenced by the binding capacity of HSA, two different HSAs were tested: one pure and one non-purified with bound FAs, which is supposed to have different binding affinities for BR. HSA does not only work as an FA transporter in the blood plasma [32,34,46,47] but FAs bound to HSA were found to play a significant role during many tasks of this protein especially in the case of drug treatment [32,34,48,49] and renal tubulointerstitial injury [50]. Additionally, even in the presence of liposomes or FA-incubated liposomes a preferential binding of FAs to HSA was observed [51,52]. Hence it is truly important to study the equilibrium in the BR/HSA/liposome system not only with pure HSA but also with albumin which was isolated from the blood plasma and which was not purified of FAs.

FAs are well-known to influence the binding capacity of HSA being its natural components and they can also transport from HSA to liposomes and vice-versa [39,51–57]. The effect of six different FAs and their mixtures was studied separately as an addition to the pure HSA solution. Since two thirds of FAs bound to HSA in the blood plasma are unsaturated under normal circumstances, the most common being oleic (OA), linoleic (LA) and arachidonic acid (AA), these three acids were selected as representatives for unsaturated FAs. For saturated FAs, the three most common FAs in the blood plasma were chosen: myristic (MA), palmitic (PA), and stearic acid (SA).

As the major method to study the described systems, the ECD spectroscopy was chosen. It enables the study of different chiral forms of bound BR (Fig. 1) and of changes in the secondary and tertiary structures of HSA as the spectral bands of HSA are in different positions from BR. The spectroscopy also enables a differentiation between BR bound to the liposomes and HSA manifested as different values of molar ellipticity and shifts in couplet positions. The spectra are also very sensitive to the changes of the dihedral angle in the BR structure (Fig. 1B). The ECD method was complemented by the UV–Vis absorption spectroscopy and by the fluorescence emission.

2. Materials and methods

2.1. Materials

The lipids 1,2-dimyristoyl-*sn*-glycero-3-phosphocholine (DMPC) and sphingomyelin were purchased from Avanti Polar Lipids (Alabaster, AL). Bilirubin-IXa (BR) was purchased from Frontier Scientific (USA). Human serum albumin (99% A3782 and 96% A1653), palmitic acid (PA), myristic acid (MA), stearic acid (SA), linoleic acid (LA), oleic acid (OA) and arachidonic acid (AA) were purchased from Sigma Aldrich. All of the chemicals were used without further purification.

2.2. Preparation of large unilamellar vesicles

The liposomes were prepared using the standard procedures [58]. The appropriate amount of dried lipid was weighed and dissolved in a chloroform/methanol mixture (2:1, v/v) and vortexed for 10 min. The sample was dried under low pressure to form a thin film on the vial wall, after which it was left under high vacuum for 5 h. The film was then hydrated via the addition of a 2×10^{-2} M phosphate buffer (pH = 7.4) and vortexed extensively for 15 min. The resulting multilamellar liposome suspension was then reduced to uniform large unilamellar vesicles (LUVs) by passing twenty-three times through a polycarbonate membrane with a mean pore diameter of 100 nm using a Mini-Extruder (Avanti Polar Lipids). After extrusion, the LUVs were allowed to equilibrate for at least 2 h before use. The final lipid concentration was calculated based on the weight of the dried lipid [59–63]. The dynamic light scattering (DLS) method confirmed the narrow size distribution of the LUVs with the maximum at approximately (110 ± 3) nm for both the DMPC and sphingomyelin liposomes.

For the testing of the scattering effects, larger liposomes (212 ± 11) nm and (415 ± 12) nm were prepared by extrusion and smaller liposomes

(80 ± 8), (50 ± 7) and (40 ± 7) nm were prepared from sphingomyelin by sonication.

2.3. Preparation of fatty acid solutions

The appropriate amount of FA was weighed, dissolved in chloroform, and vortexed for 15 min in a vial. The sample was then dried under low pressure to form a thin film on the vial wall, after which it was left under high vacuum for 4 h. The film was then hydrated with a 1×10^{-3} M solution of HSA in 2×10^{-2} M phosphate buffer (pH = 7.4) and vortexed and sonicated extensively for 80 min at 30 °C. The resulting opalescent solution was used as a bulk solution of FA and HSA. The possible effect of the procedure on the structure of HSA was inspected and found to be non-observable.

2.4. Sample preparation

The solution of a BR sodium salt (concentration 0.005 M) was prepared to achieve a higher solubility of BR [64]. Powdered BR was dissolved in a 3:1 molar excess of a sodium hydroxide aqueous solution so that a complete neutralization was achieved and the solution was centrifuged to confirm the complete dissolution of BR. This solution was used as a stock solution but for no longer than 2 h and during that time was stored in the dark and in a refrigerator. The spectral measurements were conducted in solutions of a 2×10^{-2} M phosphate buffer (pH = 7.4).

For the ECD and UV–Vis absorption measurements, the BR concentration was in the range of 1×10^{-5}–5×10^{-5} M. The concentration of the DMPC and sphingomyelin was 1×10^{-3} M. The concentration of serum albumin was in the range of 2×10^{-6}–1×10^{-5} M. The concentration of FA was 1×10^{-4} M. For the fluorescence emission measurements, the BR concentration was 1×10^{-5} M, the concentration of the DMPC and SPM liposomes was 1×10^{-3} M, and HSA concentration was 1×10^{-5} M. All the measured solutions did not show the presence of precipitates as was confirmed by their centrifugation.

2.5. Electronic circular dichroism, fluorescence emission and UV–Vis absorption

The ECD, fluorescence emission and UV–Vis absorption spectra were measured on a J-810 spectrometer equipped with a fluorescence accessory FDCD-404L (Jasco, Japan). The ECD and UV–Vis absorption spectra were measured in a quartz cuvette with an optical path length of 1 cm or 1 mm (Helma, Germany). The conditions of the measurements were as follows for the region of BR absorption: a spectral region of 250–600 nm, a scanning speed of 100 nm/min, a response time of 1 s, a resolution of 1 nm, a bandwidth of 1 nm and a sensitivity of 100 mdeg; for the region of protein absorption: a spectral region of 200–300 nm a scanning speed of 5 nm/min, a response time of 16 s, a resolution of 0.5 nm, a bandwidth of 1 nm and a sensitivity of 100 mdeg. The final spectrum was obtained as an average of 5 accumulations in both cases. Spectra are presented in molar ellipticity units relative to the concentration of BR.

The conditions of the fluorescence emission measurements were as follows: a spectral region of 460–800 nm, an excitation wavelength of 435 nm, a response time of 2 s, a resolution of 1 nm, a bandwidth of 10 nm and a sensitivity of 900 V. The final spectrum was obtained as an average of 5 accumulations. The spectra were corrected for the inner filter effect according to ref. [65].

All the measurements were conducted at room temperature (25 °C).

Liposomes of different sizes were tested (Section 2.2) to find whether there is a spectral distortion in the ECD spectra caused by the scattering from the particles. No size-related effects were observed for the tested liposomes up to 110 nm. The 110 nm liposomes were consequently used in all the measurements because of their narrow size distribution due to extrusion. For the (212 ± 11) and (415 ± 12) nm liposomes, high spectral noise accompanied with smaller distortion of the ECD bands was observed suggesting scattering effects.

3. Results and discussion

In the first part of the study, BR binding to 99% pure HSA (further called 99-HSA) and to 96% pure HSA which was not purified of FAs (hereinafter referred to as FA-HSA) and model membranes was studied. For the molecular systems composed of BR and 99-HSA, the spectral characteristics of the BR binding to HSA with and without model membranes were gained. On the other hand, the more complex molecular system with FA-HSA represented model with biological relevance. In the second part, different FAs were added to the ternary system BR/99-HSA/model membranes at the FA:HSA ratio 10:1.

All the spectra were measured after the equilibrium was reached and therefore kinetic processes should play no role in the obtained results. Measurements were done for low BR concentrations similar to physiological in the blood plasma and for the BR:lipid ratio 1:100. This ratio was used to simulate locally increased concentrations of lipids when BR is found near the cell wall. The spectra were measured for the solutions of BR into which the liposomes were added first and then, after the equilibrium was reached, HSA was added. The results obtained for the inverse course of steps did not differ considerably.

3.1. Bilirubin with 99-HSA or FA-HSA and model membranes

Figs. 2 and 3 show the ECD and UV–Vis absorption spectra obtained for the BR mixtures with the DMPC or sphingomyelin liposomes and with 99-HSA and FA-HSA, respectively. Fig. 2A summarizes the results previously obtained by us for the BR/99-HSA system [42,43]. While BR alone did not have an ECD signal because of its racemization, for 99-HSA or FA-HSA alone, a small negative band reflecting the tertiary structure was observed in the region of aromatic amino acid absorption. BR alone had a very weak fluorescence signal due to strong quenching [66,67] and, hence, only fluorescence signals of bound BR could be observed (Fig. 4).

Because only bound BR is optically active, the observed similar molar ellipticity up to the 3:1 ratio for the BR/99-HSA mixture confirmed the chiral selection of the P-form of BR into three binding sites in HSA, one primary and two secondary [42,43] (see Fig. S1 for the spectra in [mdeg] and Fig. S2 for a reversed titration). As the high value of $K_a \sim 10^8$ M^{-1} for the primary binding site indicates, more than 98% of the BR molecules in the solution were bound. The absorption spectrum of BR bound to the primary site was shifted to the red region in comparison with the spectrum of unbound BR due to the change in the torsion angle in the BR structure (Fig. 1) when bound and maybe also due to the changes in the polarity of the environment. For the ratios 2:1 and 3:1, the UV–Vis spectra were closer to the blue region indicating a shift due to different torsion angles between the secondary and primary sites. The separation of the UV–Vis spectra to the components (for details, see Section 7 of the Supplementary material) provided information about a presence of approximately 15% and 20% of unbound BR, respectively. This corresponds with the lower binging constants to the secondary binding sites. For the BR:99-HSA ratio greater than 3:1, the decrease of molar ellipticity value evidenced the saturation of an enantioselective binding of HSA towards BR.

In the case of FA-HSA (Fig. 3A, see Fig. S3 for the spectra in [mdeg] and Fig. S4 for a reversed titration), a lower value of molar ellipticity and continual decrease of signal suggested that the FAs present in the FA-HSA sample influenced the BR binding to HSA and partly hampered all three binding sites in the HSA structure. The binding possibilities of BR were more limited in this system when compared with 99-HSA. Separation of the UV–Vis spectra to the components led to the estimation of 10% of unbound BR for the 1:1 ratio. This was confirmed by the lower intensity in the fluorescence emission compared to BR with 99-HSA (Fig. 4).

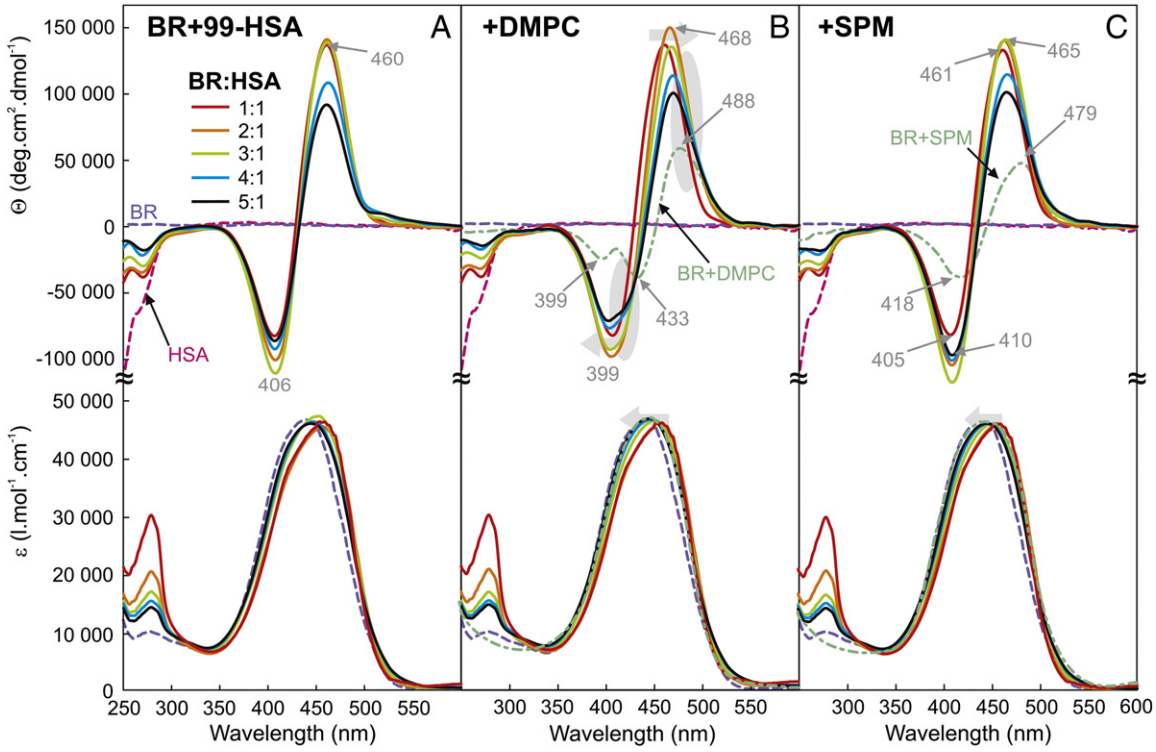

Fig. 2. The ECD (top) and UV–Vis spectra (bottom) of BR with 99-HSA (A) and in the presence of the DMPC (B) or sphingomyelin (SPM) liposomes (C) measured for the BR:99-HSA ratios from 1:1 to 5:1. The spectra of 99-HSA (A), BR (all panels) and BR with the DMPC (B) or sphingomyelin liposomes (C) are also shown. The concentration of 99-HSA was 1×10^{-5} M, that of the liposomes 1×10^{-3} M and the BR concentration was given by the BR:99-HSA ratio and was in the region of 1×10^{-5} M–5×10^{-5} M.

Both studied types of liposomes interacted with BR enantioselectively, they recognized the same P-conformer [29], however with a different position and intensity (Figs. 2B,C, 3B,C) than in the BR/HSA system. As the position and intensity of the BR couplet strongly depend on the dihedral angle in the BR structure [68] (schematically shown in Fig. 1), we suppose that the structure of BR interacting with the liposomes was different from

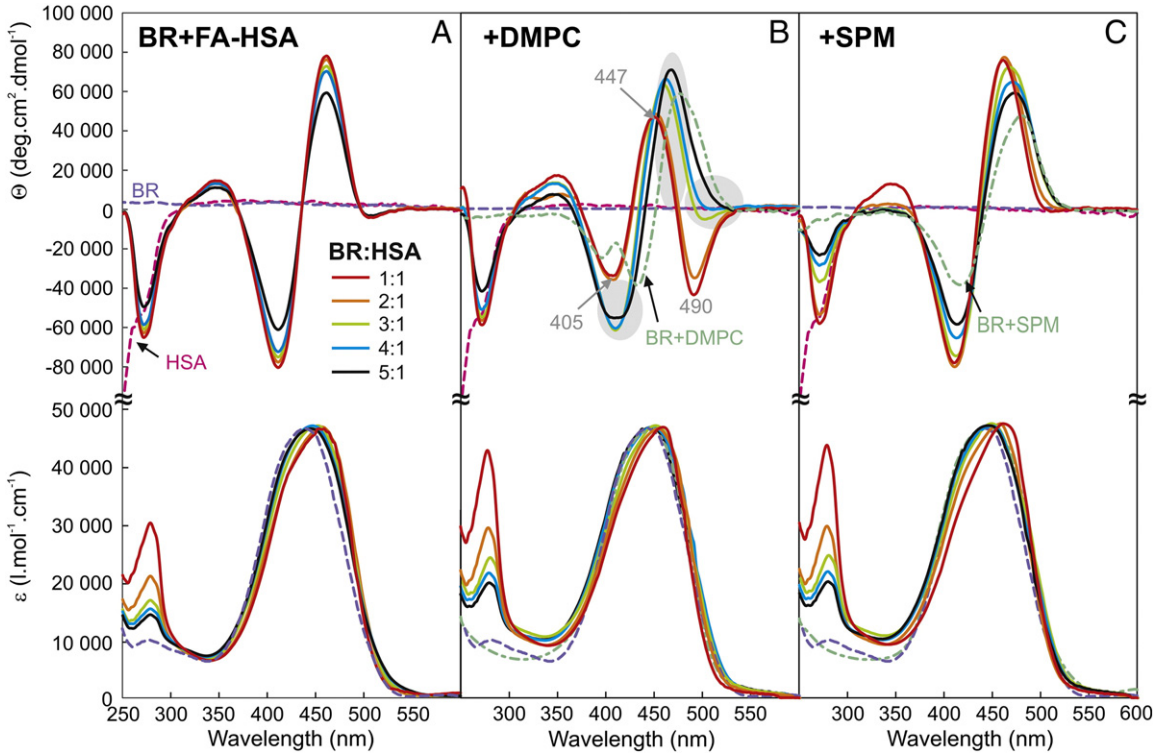

Fig. 3. The ECD (top) and UV–Vis spectra (bottom) of BR with FA-HSA (A) and in the presence of the DMPC (B) or sphingomyelin (SPM) liposomes (C) measured for the BR:FA-HSA ratios from 1:1 to 5:1. The spectra of FA-HSA (A), BR (all panels) and BR with the DMPC (B) or sphingomyelin liposomes (C) are also shown. The concentration of FA-HSA was 1×10^{-5} M, that of the liposomes 1×10^{-3} M and the BR concentration was given by the BR:FA-HSA ratio and was in the region of 1×10^{-5} M–5×10^{-5} M.

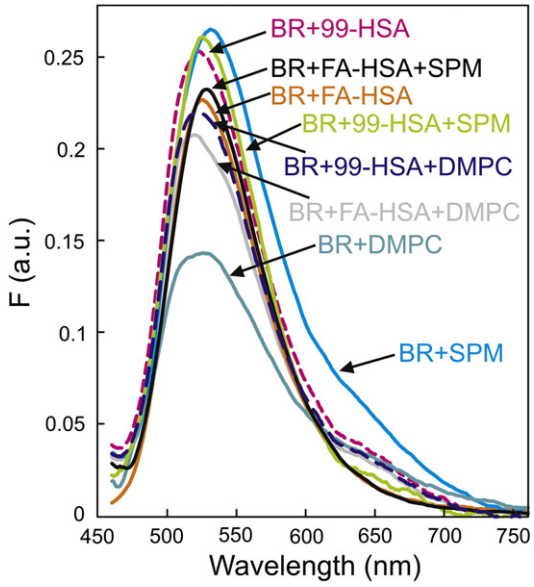

Fig. 4. The fluorescence emission spectra of BR with 99-HSA and FA-HSA and in the presence of the DMPC or sphingomyelin (SPM) liposomes. The spectra of the ternary mixture of BR/99-HSA/liposomes and BR/FA-HSA/liposomes are also shown. All the spectra were measured for the BR:HSA ratio 1:1. The concentration of HSA and BR was 1×10^{-5} M and of the liposomes was 1×10^{-3} M.

the one observed for the binding to 99-HSA and to FA-HSA. The shift of the couplet position and the shift observed in the fluorescence spectra also evidenced the influence of different polarity of the environment, especially, in the case of the DMPC liposomes where BR bound deeper into the bilayer [29].

The impact of the DMPC liposomes on the BR binding to 99-HSA and FA-HSA was very different (cf. Figs. 2B and 3B). For the 1:1 BR:99-HSA ratio, the minor spectral changes caused by the presence of DMPC liposomes suggested that liposomes did not compete with the primary binding site of 99-HSA. The analyses of the fluorescence emission spectra (for details, see Section 7 of Supplementary material and Table S2) show only 10% and 8% of bound BR bound to the DMPC and sphingomyelin liposomes, respectively. The UV–Vis spectra evidenced similar results and only about 4% of unbound BR.

However, already for the BR:99-HSA ratio 2:1, the molar ellipticity increased, both components of the couplet were broader and a shift of the couplet position quoted in Fig. 2 was observed. Although the spectral effects of the liposome presence are not very pronounced, it is clear that at increased BR concentrations, which accompany several pathologic states in the human body, competition between the secondary sites and liposomes occurred after the saturation of the primary binding site, and BR bound to both 99-HSA and liposomes. Interestingly, as the shifts in the UV–Vis spectra and their separation to the components suggested, BR bound more to the DMPC liposomes than to the sphingomyelin liposomes (~48 and ~44% of bound BR, respectively, Table S1). For the higher ratios, an increase of the unbound BR was observed as well as its binding to the liposomes.

In the case of FA-HSA, the presence of the DMPC liposomes caused a distinctly different response already at BR:FA-HSA ratio 1:1 as is depicted in Fig. 3B. The observed spectral pattern with a new presence of a higher-wavelength negative band was probably a result of overlapping couplets for the P- and M-forms of BR with different positions of the couplets, which is usually an effect of different torsion angles in the BR structure (ref. [68] and Fig. 1). This suggested that not only the P-form but also the M-form of BR bound to FA-HSA. The possible explanation might be that the presented FAs influenced the DMPC liposomes and hence the M-form of BR bound onto them. However, the liposomes prepared from DMPC, MA, PA and SA did not show any changes in the enantioselectivity of the BR binding (Fig. S5). Also, the same FAs added to the BR solution with the DMPC liposomes did not change the BR signal. This means that the influence of the DMPC liposomes and FAs from FA-HSA led to changes in the HSA primary binding site so that the M-form of BR also bound. Also the analysis of the fluorescence and UV–Vis spectra (Tables S1 and S2) provided ~27–32% of bound BR bound to the DMPC liposomes, which was more than three times higher when compared to the 99-HSA system.

The differences in intensity for all ratios in comparison with the 99-HSA system were connected to the effect of FAs from FA-HSA. They probably blocked one or both of the secondary binding sites of HSA. That supported more BR binding to the DMPC liposomes as was also confirmed by the separation of the UV–Vis absorption bands for the higher ratios (approximately 63% for BR bound to the liposomes relative to the secondary sites of FA-HSA for the 3:1 ratio).

The influence of the sphingomyelin liposomes is depicted in Figs. 2C and 3C. For both 99-HSA and FA-HSA systems, the sphingomyelin liposomes affected the binding of BR to HSA even at the ratio favoring the primary binding site (~26% of bound BR bound to the liposomes, Tables S1 and S2). As far as the secondary binding sites were concerned, BR preferred to bind to the liposomes in the FA-HSA system more times than in the 99-HSA system (~60% for FA-HSA and ~44% for 99-HSA of BR bound to the liposomes Table S1). However, unlike the system with the DMPC liposomes, no inversion of the BR conformation upon binding was observed.

The obtained results indicated that FAs, which form an inherent part of the HSA transporter in the human blood plasma, significantly influence HSA interaction with BR and may contribute to its binding to membranes. Remarkably, BR significantly bound to the sphingomyelin liposomes at higher concentrations and even at the BR:HSA ratio 1:1 typical for the blood plasma. The combined effect of FAs from FA-HSA and of the DMPC liposomes caused changes in the FA-HSA primary binding site and supported more BR binding to the liposomes. This means that especially at increased BR concentrations, BR would not bind dominantly to HSA but would also bind to cell membranes, and this may lead to damage of the cell structure.

All the described molecular systems were tested also for a reversed titration (Figs. S2 and S4), which confirmed the observations made above.

3.2. Bilirubin with 99-HSA, fatty acids and model membranes

As we have described in the previous part, the interactions in the system with FA-HSA differed greatly from the system with 99-HSA indicating the potential negative biological effects of BR on cell membranes. Therefore, we tried to identify which of the most abundant FAs in the blood plasma, three saturated and three unsaturated, had the biggest impact. Since at least seven binding sites of FAs were described in the structure of HSA [31,32], a 10:1 excess of FAs over HSA was used.

3.2.1. The effect of saturated fatty acids

The influence of MA, PA and SA and of their equimolar mixture was studied. As the effect of each individual FA was similar, here we show only the results obtained for PA (Fig. 5) and the mixture of PA, MA and SA (Fig. 6).

The spectra reported in Fig. 5A depict the influence of PA on the BR binding to 99-HSA without liposomes. The observed spectral pattern for the BR:99-HSA ratio 1:1 (in accordance with ref. [69]) indicated that in the presence of PA not only the P-form but also the M-form of BR bound to the primary site of HSA. The couplets for the M- and P-forms overlapped and the resulting signal did not have an apparent positive maximum (Fig. 1). Similar effects were also observed in the presence of MA and SA and the mixture of saturated FAs (Figs. S6, S7 and 6).

For the increasing ratios, where the primary site and the secondary sites might be involved, the P-form prevailed implying that the enantioselectivity of the secondary binding sites was not gravely influenced. The UV–Vis spectra were shifted more to the red region in

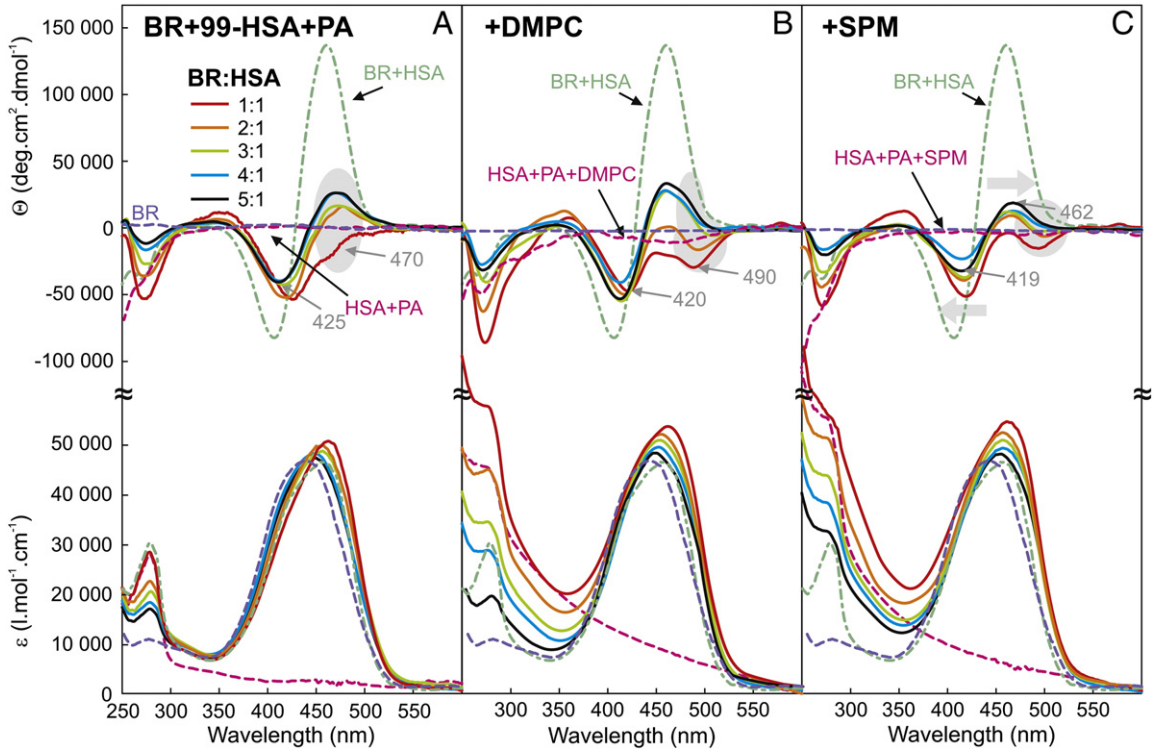

Fig. 5. The ECD (top) and UV–Vis spectra (bottom) of BR with PA and 99-HSA (A) and in the presence of the DMPC (B) or sphingomyelin (SPM) liposomes (C) measured for the BR:99-HSA ratios from 1:1 to 5:1. The spectra of 99-HSA with BR (ratio 1:1, all panels), 99-HSA with PA (A) and with the DMPC (B) or sphingomyelin (SPM) liposomes (C) are also shown. The concentration of 99-HSA was 1×10^{-5} M, that of PA 1×10^{-4} M, that of the liposomes 1×10^{-3} M and the BR concentration was given by the BR:99-HSA ratio and was in the region of 1×10^{-5} M–5×10^{-5} M.

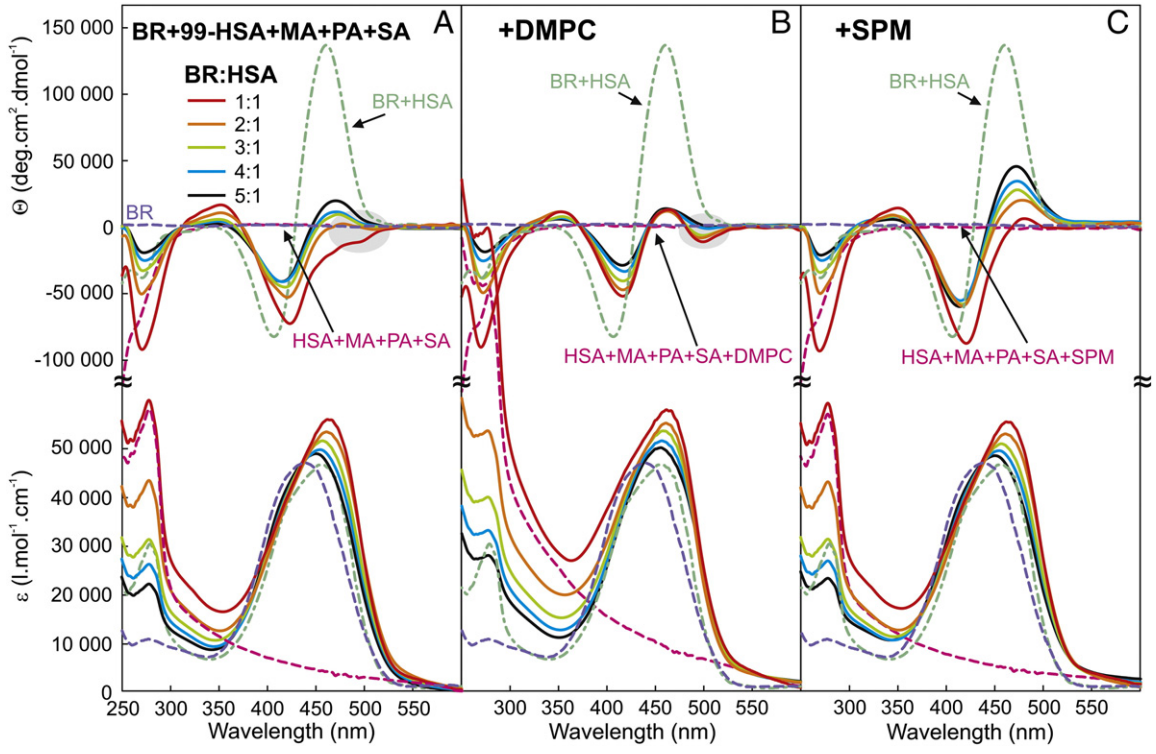

Fig. 6. The ECD (top) and UV–Vis spectra (bottom) of BR with PA, MA, and SA mixture (1:1:1) and 99-HSA (A) and in the presence of the DMPC (B) or sphingomyelin (SPM) liposomes (C) measured for the BR:99-HSA ratios from 1:1 to 5:1. The spectra of 99-HSA with BR (ratio 1:1, all panels), 99-HSA with PA, MA, and SA mixture (1:1:1) (A) and with the DMPC (B) or sphingomyelin (SPM) liposomes (C) are also shown. The concentration of 99-HSA was 1×10^{-5} M, that of the liposomes 1×10^{-3} M and the BR concentration was given by the BR:99-HSA ratio and was in the region of 1×10^{-5} M–5×10^{-5} M. The total concentration of FAs was 1×10^{-4} M.

comparison with 99-HSA system probably due to the different dihedral angles of the M-form of BR and due to the presence of FAs influencing the polarity of the environment.

Interestingly, the molar ellipticity in this system was very low compared to the system without FAs (cf. Figs. 5 and 2); most likely, because saturated FAs limited the binding possibilities of BR to all three binding sites. This was confirmed by the analysis of the UV–Vis spectra which showed 10% and 31% of unbound BR for the 1:1 and 3:1 ratios, respectively (Table S1). However, because each acid has a different chain length, each of them caused a specific hindrance of the BR binding. The molar ellipticity was the lowest for the shortest of the studied FAs MA. The binding possibilities of MA in 99-HSA were greater and hence it hampered the binding sites of 99-HSA more. This was also confirmed by the highest fraction of unbound BR 14% for the 1:1 ratio and by the observed changes in the secondary structure of HSA which were reflected in the 200–300 nm region of the ECD spectra. According to our deconvolution of the spectra using CDNN software (developed by Gerald Bohm of the University of Halle, Germany [70]), MA decreased the apparent content of the α-helical conformation of 99-HSA more than PA and SA (Table S3).

The system composed of the DMPC liposomes with PA is shown in Fig. 5B and with the saturated FA mixture in Fig. 6B. The observed spectra were similar to the FA-HSA system suggesting the binding of both the P- and M-forms of BR to the primary site of 99-HSA. The low intensity of the spectra indicated that the affinity of FAs towards 99-HSA was higher than towards the liposomes [52,55,71,72] and they hindered part of the primary sites of 99-HSA (~34% of BR bound to the DMPC liposomes and only ~66% to the primary site, Table S2). The UV–Vis spectra showed approximately 8% of unbound BR (Table S1).

The complex ECD spectral shape for higher ratios suggested an overlap of three spectral components: of the BR bound to the primary site, of the BR bound to the secondary sites of 99-HSA, and of the BR bound to the DMPC liposomes (a model summation of the components in Fig. S8). The enantioselective binding to the secondary sites was limited, because the overall spectral intensity was very low — over 30% of unbound BR according to the analysis of the UV–Vis spectra. This indicated a preference for the BR binding to the liposomes confirmed also by the UV–Vis spectra (~67% of bound BR was bound to the liposomes, Table S1). Remarkably, this was observed to a greater extent in the system with the saturated FA mixture than with individual FAs.

The situation for the sphingomyelin liposomes with PA is depicted in Fig. 5C, with the mixture of saturated FAs in Fig. 6C. For the BR:99-HSA ratio 1:1, there was an indication of the M-form of BR bound to 99-HSA but the P-form prevailed. With the increasing ratios, BR bound in the P-form to the secondary sites of 99-HSA and also to the liposomes. All saturated FAs caused a blue shift of the couplet for BR bound to 99-HSA, as a result of the conformational change of bound BR, while they had no effect on the BR binding to the sphingomyelin liposomes (Fig. S5). Interestingly, as the analyses of the UV–Vis spectra show, binding to the sphingomyelin liposomes was even more pronounced in the systems with MA and SA than with PA; ~66% for BR bound to the liposomes for PA, 69% for MA and 65% for SA.

The combination of saturated FAs and also each individual saturated FA strongly influenced BR binding to the primary site of 99-HSA for which they changed the stereoselectivity of BR binding. They also limited the binding to the secondary sites probably due to their presence in the sites [30,31,34]. This fact favored the BR binding to the liposomes which was strongly evidenced for both types of liposomes. The obtained spectra shared common features with the spectra obtained in the presence of FA-HSA indicating that saturated FAs play role during BR interactions with serum albumin in the blood plasma and support BR binding to the membranes.

3.2.2. The effect of unsaturated fatty acids

The impact of unsaturated FAs on the BR interactions with 99-HSA both without and in the presence of the liposomes is demonstrated for AA in Fig. 7. In the system without liposomes, a very weak ECD signal in the BR region was observed. Similar spectra were also observed in the case of LA and OA (Fig. S9). Zero fluorescence was also observed for all three FAs. The BR racemate probably interacted with the unsaturated FAs. This was demonstrated in the UV–Vis spectra (Figs. 7 and S9) where a significant band at 483 nm was observed independently of the presence of 99-HSA. This indicated nearly 100% of unbound BR. Hence, the structure of BR was strongly affected by unsaturated FAs. The effect on 99-HSA was minimal, which was observed in the spectral region reflecting its tertiary (Figs. 7 and S9) and secondary structures (spectra not shown).

In the presence of AA and the DMPC or sphingomyelin liposomes (Figs. 7B and C), BR interacted enantioselectively. For both the liposomes, the UV–Vis spectral band separation showed that BR bound mostly to the liposomes (40% for the 1:1 and 70% for the 3:1 ratio) and only slightly to 99-HSA. The UV–Vis spectral band at 483 nm was not seen in the presence of liposomes. This means that free AA bound to BR in the system without liposomes and disabled BR binding to 99-HSA. Yet, in the presence of the liposomes, AA bound to the liposomes and did not interact significantly with BR. Hence, BR could bind to the liposomes and also moderately to mainly the primary site of 99-HSA. Interestingly, the interaction of OA and LA with BR was stronger than with the liposomes, so nearly no signal was observed in the ECD spectra (Fig. S9).

3.2.3. Combined effect of saturated and unsaturated fatty acids

Fig. 8A shows that the combined effect of an equimolar mixture of all the studied FAs was comparable to the unsaturated FAs, so that BR almost did not bind to 99-HSA. This was also confirmed by the UV–Vis absorption and fluorescence emission spectra. The ECD spectra in the presence of liposomes showed an enantioselective binding of BR and the spectral envelope reflected BR binding both to the liposomes and to the primary and secondary sites of 99-HSA. The observed results suggested that the effect of the unsaturated acids in the mixture was more significant than the effect of the saturated acids. Generally, the spectra were most similar to the spectra measured with AA, which confirms the importance of this acid in human plasma. Overall, the presence of saturated and unsaturated FAs either in combination or alone strongly restricts the BR binding to 99-HSA and supports its binding to the model membranes. Although the used FAs are among the most abundant in the blood plasma, they are not present in the same concentrations. This probably caused the discrepancy between the spectra for FA-HSA (Fig. 3) and for the FA mixture (Fig. 8). It is probable that under physiological conditions, the unsaturated FAs do not influence BR binding to HSA to such an extent.

4. Conclusions

In this study, the effect of model membranes on the BR binding to HSA was demonstrated. The results obtained in the presence of highly purified 99-HSA suggested that at low BR concentrations, typical of the blood plasma of a healthy human, BR preferred to bind to the primary binding site of 99-HSA. For the increased concentrations of BR, simulating pathologic states, a minor binding of BR to the liposomes was observed but a strong preference for the binding sites of 99-HSA was documented.

However, for the non-purified FA-HSA, a remarkable effect of both the DMPC and sphingomyelin liposomes on the BR binding to FA-HSA was manifested. For the DMPC liposomes, even competition with the primary binding site of HSA occurred and the combined effect of FAs and the DMPC liposomes caused changes in the conformation of bound BR. For higher BR concentrations, the BR binding to both the primary and secondary sites of FA-HSA and the DMPC liposomes was observed. On the other hand, the effect of the sphingomyelin liposomes on the BR binding to the primary site of FA-HSA was negligible

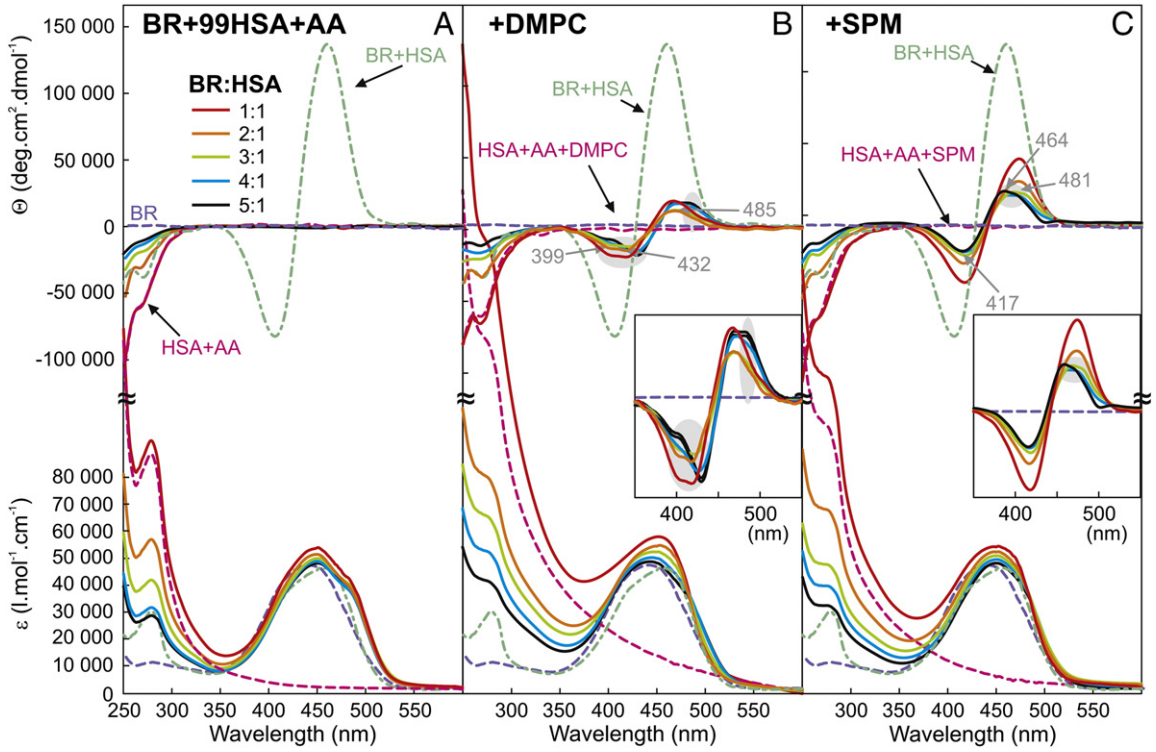

Fig. 7. The ECD (top) and UV–Vis spectra (bottom) of BR with AA and 99-HSA (A) and in the presence of the DMPC (B) or sphingomyelin (SPM) liposomes (C) measured for the BR:99-HSA ratios from 1:1 to 5:1. The spectra of 99-HSA with BR (ratio 1:1, all panels), 99-HSA with AA (A) and with the DMPC (B) or sphingomyelin (SPM) liposomes (C) are also shown. The concentration of 99-HSA was 1×10^{-5} M, that of the liposomes 1×10^{-3} M and the BR concentration was given by the BR:99-HSA ratio and was in the region of 1×10^{-5} M–5×10^{-5} M. The concentration of AA was 1×10^{-4} M.

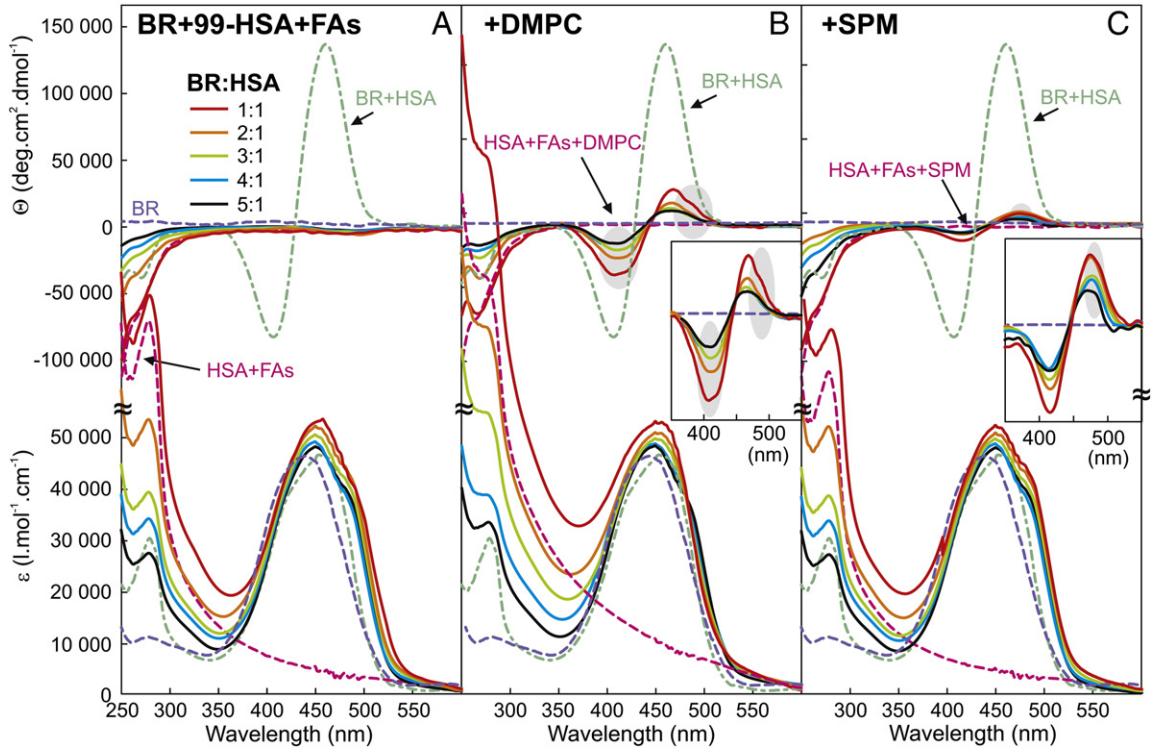

Fig. 8. The ECD (top) and UV–Vis spectra (bottom) of BR with MA, PA, SA, LA, OA and AA mixture (1:1:1:1:1:1) and 99-HSA (A) and in the presence of the DMPC (B) or sphingomyelin (SPM) liposomes (C) measured for the BR:99-HSA ratios from 1:1 to 5:1. The spectra of 99-HSA with BR (ratio 1:1, all panels), 99-HSA with MA, PA, SA, LA, OA and AA mixture (1:1:1:1:1:1) (A) and with the DMPC (B) or sphingomyelin (SPM) liposomes (C) are also shown. The concentration of 99-HSA was 1×10^{-5} M, that of the liposomes 1×10^{-3} M and the BR concentration was given by the BR:99-HSA ratio and was in the region of 1×10^{-5} M–5×10^{-5} M. The concentration of MA, PA, SA, LA, OA and AA mixture (1:1:1:1:1:1) was 1×10^{-4} M.

while they competed with the secondary sites more than the DMPC liposomes.

The observed effects of the combination of the liposomes and FAs presented in the FA-HSA sample were explained with the study of liposomic solutions with the individual FAs and 99-HSA. We may conclude that the effect of the added FAs on the BR binding to 99-HSA and model membranes was stronger than for the FAs presented as a component of FA-HSA. The saturated FAs and their mixture influenced the BR binding to 99-HSA and liposomes in a similar way as the FAs from FA-HSA. Nevertheless, a stronger effect for lower concentrations of BR was observed. The effect of unsaturated FAs, which are more common in the human blood plasma, was quite unexpected and not very similar to what was observed for FA-HSA. They interacted with BR and prevented it from interacting with both 99-HSA and liposomes. Only in the presence of AA, BR interacted enantioselectively with the liposomes and 99-HSA.

As the spectra observed in the presence of both the DMPC and sphingomyelin liposomes with FA-HSA were similar to the spectra measured in the presence of the combination of all the FAs, we suggest that all of the different types of FAs contribute in a different extent. When FAs naturally occur in the HSA structure (FA-HSA), they do not influence its structure so gravely and do not disturb BR binding as much as when we added them to the solution. Most likely, they were not released from the FA-HSA structure so effortlessly in order to interact with BR and prevent it from binding to FA-HSA. This also showed that the effect of FAs which are found in the blood plasma and of FAs which are transported as bound to HSA is different.

Hence, we may conclude that primarily the saturated FAs have an impact on the BR interactions in the solutions with FA-HSA. Also as a result of the FA occurrence in the blood plasma and in the natural structure of HSA, BR may possibly bind to cell membranes even though it is primarily bound to HSA. The probability of this increases with BR concentration and the presence of saturated FAs and is dependent on the type of lipids in the membranes. Therefore, we confirmed that, at increased BR concentrations or during its accumulation in tissues, BR binding to cell membranes is possible and, hence, is also the supposed neurotoxicity of BR.

Transparency document

The Transparency document associated with this article can be found, in the online version.

Acknowledgement

Financial support from Specific University Research MSMT No 20/2014 (A2_FCHI_2014_011; A1_FCHI_2014_003) and MSMT No 20/2013 (A2_FCHI_2013_010; A1_FCHI_2013_003) and by the Czech Science Foundation (P206/11/0836, P208/11/0105) is gratefully acknowledged. Supported by "Operational Program Prague — Competitiveness" (CZ.2.16/3.1.00/22197) and "National Program of Sustainability" (NPU I (LO) MSMT — 34870/2013).

Appendix A. Supplementary data

Supplementary data to this article can be found online at http://dx.doi.org/10.1016/j.bbamem.2015.02.026.

References

[1] D. Voet, J.G. Voet, Biochemistry, Wiley, New York, 2004.
[2] S.E. Boiadjiev, D.A. Lightner, Exciton chirality of bilirubin homologs, Chirality 9 (1997) 604–615.
[3] S.E. Boiadjiev, D.A. Lightner, Optical activity and stereochemistry of linear oligopyrroles and bile pigments, Tetrahedron Asymmetry 10 (1999) 607–655.
[4] S.E. Boiadjiev, R.V. Person, G. Puzicha, C. Knobler, E. Maverick, K.N. Trueblood, D.A. Lightner, Absolute-configuration of bilirubin conformational enantiomers, J. Am. Chem. Soc. 114 (1992) 10123–10133.
[5] R.V. Person, B.R. Peterson, D.A. Lightner, Bilirubin conformational-analysis and circular-dichroism, J. Am. Chem. Soc. 116 (1994) 42–59.
[6] L. Vitek, J.D. Ostrow, Bilirubin chemistry and metabolism; harmful and protective aspects, Curr. Pharm. Des. 15 (2009) 2869–2883.
[7] L. Vitek, L. Sedlackova, P. Branny, T. Ruml, Metabolism of bilirubin and methods of elimination of its toxicity, Chem. List. 97 (2002) 24–28.
[8] M.A. Brito Brites, D. Matos, R.F.M. Silva, Comparative study of adverse effects of hyperbilirubinaemia on foetal and adult erythrocytes, Influence of acidosisJ. Hepatol. 34 (2001) 181-181.
[9] M.A. Brito, D. Brites, D.A. Butterfield, A link between hyperbilirubinemia, oxidative stress and injury to neocortical synaptosomes, Brain Res. 1026 (2004) 33–43.
[10] M.J. Daood, A.F. McDonagh, J.F. Watchko, Calculated free bilirubin levels and neurotoxicity, J. Perinatol. 29 (2009) S14–S19.
[11] J.D. Ostrow, L. Pascolo, D. Brites, C. Tiribelli, Molecular basis of bilirubin-induced neurotoxicity, Trends Mol. Med. 10 (2004) 65–70.
[12] L. Rigato, J.D. Ostrow, C. Tiribelli, Bilirubin and the risk of common non-hepatic diseases, Trends Mol. Med. 11 (2005) 277–283.
[13] D.K. Stevenson, H.J. Vreman, R.J. Wong, Bilirubin production and the risk of bilirubin neurotoxicity, Semin. Perinatol. 35 (2011) 121–126.
[14] A.K. Masood, S.M. Faisal, M.K. Mushahid, A. Nadeem, M.U. Siddiqui, M. Owais, Binding of bilirubin with albumin-coupled liposomes: implications in the treatment of jaundice, BBA-Biomembranes 1564 (2002) 219–226.
[15] D. Brites, The evolving landscape of neurotoxicity by unconjugated bilirubin: role of glial cells and inflammation, Front. Pharmacol. 3 (2012) 88.
[16] M.A. Brito, C.D. Brondino, J.J.G. Moura, D. Brites, Effects of bilirubin molecular species on membrane dynamic properties of human erythrocyte membranes: a spin label electron paramagnetic resonance spectroscopy study, Arch. Biochem. Biophys. 387 (2001) 57–65.
[17] P. Mukerjee, J.D. Ostrow, Review: Bilirubin pKa studies; new models and theories indicate high pKa values in water, dimethylformamide and DMSO, BMC Biochem. 11 (2010).
[18] C. Bernardini, P. D'Arrigo, G. Elemento, G. Mancini, S. Servi, A. Sorrenti, The possible role of enantiodiscrimination in bilirubin toxicity, Chirality 21 (2009) 87–91.
[19] S. Borocci, F. Ceccacci, O. Cruciani, G. Mancini, A. Sorrenti, Chiral recognition in biomembrane models: what is behind a 'simple model', Synlett (2009) 1023–1033.
[20] A. Sorrenti, B. Altieri, F. Ceccacci, P. Profio, R. Germani, L. Giansanti, G. Savelli, G. Mancini, Deracemization of bilirubin as the marker of the chirality of micellar aggregates, Chirality 24 (2012) 78–85.
[21] S.D. Zucker, W. Goessling, Bilirubin-membrane interactions: bilayer localization of unconjugated and taurine-conjugated bilirubin as determined by parallax analysis of fluorescence quenching, Hepatology 32 (2000) 427a-427a.
[22] S.D. Zucker, W. Goessling, E.J. Bootle, C. Sterritt, Localization of bilirubin in phospholipid bilayers by parallax analysis of fluorescence quenching, J. Lipid Res. 42 (2001) 1377–1388.
[23] S.D. Zucker, W. Goessling, A.G. Hoppin, Unconjugated bilirubin exhibits spontaneous diffusion through model lipid bilayers and native hepatocyte membranes, J. Biol. Chem. 274 (1999) 10852–10862.
[24] S.D. Zucker, A.G. Hoppin, Unconjugated bilirubin exhibits spontaneous transmembrane flip-flop, Hepatology 24 (1996) 22-22.
[25] M.A. Brito, R. Silva, C. Tiribelli, D. Brites, Assessment of bilirubin toxicity to erythrocytes. Implication in neonatal jaundice management, Eur. J. Clin. Invest. 30 (2000) 239–247.
[26] D.A. Lightner, J.K. Gawronski, W.M.D. Wijekoon, Complementarity and chiral recognition — enantioselective complexation of bilirubin, J. Am. Chem. Soc. 109 (1987) 6354–6362.
[27] S.B. Amin, Effect of free fatty acids on bilirubin–albumin binding affinity and unbound bilirubin in premature infants, J. Parenter. Enter. Nutr. 34 (2010) 414–420.
[28] H.J. Verkade, M.A.C. De Bruijn, M.A. Brink, H. Talsma, R.J. Vonk, F. Kuipers, A.K. Groen, Interactions between organic anions, micelles and vesicles in model bile systems, Biochem. J. 320 (1996) 917–924.
[29] P. Novotna, I. Goncharova, M. Urbanova, Mutual structural effect of bilirubin and model membranes by vibrational circular dichroism, BBA-Biomembranes 1838 (2014) 831–841.
[30] A.A. Bhattacharya, T. Grüne, S. Curry, Crystallographic analysis reveals common modes of binding of medium and long-chain fatty acids to human serum albumin, J. Mol. Biol. 303 (2000) 721–732.
[31] J.R. Simard, P.A. Zunszain, J.A. Hamilton, S. Curry, Location of high and low affinity fatty acid binding sites on human serum albumin revealed by NMR drug-competition analysis, J. Mol. Biol. 361 (2006) 336–351.
[32] I. Petitpas, T. Grüne, A.A. Bhattacharya, S. Curry, Crystal structures of human serum albumin complexed with monounsaturated and polyunsaturated fatty acids, J. Mol. Biol. 314 (2001) 955–960.
[33] G.V. Richieri, A.M. Kleinfeld, Unbound free fatty acid levels in human serum, J. Lipid Res. 36 (1995) 229–240.
[34] S. Curry, P. Brick, N.P. Franks, Fatty acid binding to human serum albumin: new insights from crystallographic studies, BBA — Mol. Cell Biol. Lipids 1441 (1999) 131–140.
[35] J. Jacobsen, R. Brodersen, Albumin–bilirubin binding mechanism. Kinetic and spectroscopic studies of binding of bilirubin and xanthobilirubic acid to human serum albumin, J. Biol. Chem. 258 (1983) 6319–6326.
[36] A. Knudsen, A.O. Pedersen, R. Brodersen, Spectroscopic properties of bilirubin–human serum albumin complexes: a stoichiometric analysis, Arch. Biochem. Biophys. 244 (1986) 273–284.

[37] R.A. Weisiger, J.D. Ostrow, R.K. Koehler, C.C. Webster, P. Mukerjee, L. Pascolo, C. Tiribelli, Affinity of human serum albumin for bilirubin varies with albumin concentration and buffer composition: results of a novel ultrafiltration method, J. Biol. Chem. 276 (2001) 29953–29960.
[38] A. Sri Ranjini, P.K. Das, P. Balaram, Binding constant measurement by hyper-rayleigh scattering: bilirubin–human serum albumin binding as a case study, J. Phys. Chem. B 109 (2005) 5950–5953.
[39] C.B. Berde, B.S. Hudson, R.D. Simoni, L.A. Sklar, Human serum albumin. Spectroscopic studies of binding and proximity relationships for fatty acids and bilirubin, J. Biol. Chem. 254 (1979) 391–400.
[40] P.A. Zunszain, J. Ghuman, A.F. McDonagh, S. Curry, Crystallographic analysis of human serum albumin complexed with 4Z,15E-bilirubin-IXα, J. Mol. Biol. 381 (2008) 394–406.
[41] C.E. Petersen, C.E. Ha, K. Harohalli, J.B. Feix, N.V. Bhagavan, A dynamic model for bilirubin binding to human serum albumin, J. Biol. Chem. 275 (2000) 20985–20995.
[42] I. Goncharova, S. Orlov, M. Urbanova, Chiroptical properties of bilirubin–serum albumin binding sites, Chirality 25 (2013) 257–263.
[43] I. Goncharova, S. Orlov, M. Urbanova, The location of the high- and low-affinity bilirubin-binding sites on serum albumin: ligand-competition analysis investigated by circular dichroism, Biophys. Chem. 180 (2013) 55–65.
[44] M. Leonard, N. Noy, D. Zakim, The interactions of bilirubin with model and biological membranes, J. Biol. Chem. 264 (1989) 5648–5652.
[45] N. Noy, M. Leonard, D. Zakim, The kinetics of interactions of bilirubin with lipid bilayers and with serum albumin, Biophys. Chem. 42 (1992) 177–188.
[46] A.A. Spector, Fatty acid binding to plasma albumin, J. Lipid Res. 16 (1975) 165–179.
[47] S. Sugio, A. Kashima, S. Mochizuki, M. Noda, K. Kobayashi, Crystal structure of human serum albumin at 2.5 Å resolution, Protein Eng. 12 (1999) 439–446.
[48] J.D. Ashbrook, A.A. Spector, E.C. Santos, J.E. Fletcher, Long chain fatty acid binding to human plasma albumin, J. Biol. Chem. 250 (1975) 2333–2338.
[49] J. Reynolds, S. Herbert, J. Steinhardt, The binding of some long-chain fatty acid anions and alcohols by bovine serum albumin, Biochemistry 7 (1968) 1357–1361.
[50] J. Nagai, A. Yamamoto, Y. Katagiri, R. Yumoto, M. Takano, Fatty acid-bearing albumin but not fatty acid-depleted albumin induces HIF-1 activation in human renal proximal tubular epithelial cell line HK-2, Biochem. Biophys. Res. Commun. 450 (2014) 476–481.
[51] P. Brecher, R. Saouaf, J.M. Sugarman, D. Eisenberg, K. LaRosa, Fatty acid transfer between multilamellar liposomes and fatty acid-binding proteins, J. Biol. Chem. 259 (1984) 13395–13401.
[52] M. Pantusa, R. Bartucci, Kinetics of stearic acid transfer between human serum albumin and sterically stabilized liposomes, Eur. Biophys. J. 39 (2010) 1351–1357.
[53] I.N. Bojesen, E. Bojesen, Binding of arachidonate and oleate to bovine serum albumin, J. Lipid Res. 35 (1994) 770–778.
[54] E. Bojesen, I.N. Bojesen, Albumin binding of long-chain fatty acids: thermodynamics and kinetics, J. Phys. Chem. 100 (1996) 17981–17985.
[55] J.K. Ho, H. Moser, Y. Kishimoto, J.A. Hamilton, Interactions of a very long chain fatty acid with model membranes and serum albumin: Implications for the pathogenesis of adrenoleukodystrophy, J. Clin. Invest. 96 (1995) 1455–1463.
[56] J.K. Choi, J. Ho, S. Curry, D. Qin, R. Bittman, J.A. Hamilton, Interactions of very long-chain saturated fatty acids with serum albumin, J. Lipid Res. 43 (2002) 1000–1010.
[57] J. Jacobsen, H. Theissen, R. Brodersen, Effect of fatty acids on the binding of bilirubin to albumin, Biochem. J. 126 (1972).
[58] V. Torchilin, V. Weissig, in: V. Torchilin, V. Weissig (Eds.), Liposomes, Oxford University Press, New York, 2003, pp. 3–8.
[59] A.L. Russell, A.M. Kennedy, A.M. Spuches, D. Venugopal, J.B. Bhonsle, R.P. Hicks, Spectroscopic and thermodynamic evidence for antimicrobial peptide membrane selectivity, Chem. Phys. Lipids 163 (2010) 488–497.
[60] S.Y. Wen, M. Majerowicz, A. Waring, F. Bringezu, Dicynthaurin (ala) monomer interaction with phospholipid bilayers studied by fluorescence leakage and isothermal titration calorimetry, J. Phys. Chem. B 111 (2007) 6280–6287.
[61] T. Wieprecht, O. Apostolov, M. Beyermann, J. Seelig, Membrane binding and pore formation of the antibacterial peptide PGLa: thermodynamic and mechanistic aspects, Biochemistry 39 (2000) 442–452.
[62] O. Wieprecht, J. Apostolov, Seelig, Binding of the antibacterial peptide magainin 2 amide to small and large unilamellar vesicles, Biophys. Chem. 85 (2000) 187–198.
[63] T. Wieprecht, M. Beyermann, J. Seelig, Thermodynamics of the coil-alpha-helix transition of amphipathic peptides in a membrane environment: the role of vesicle curvature, Biophys. Chem. 96 (2002) 191–201.
[64] I. Goncharova, M. Urbanova, Bile pigment complexes with cyclodextrins: electronic and vibrational circular dichroism study, Tetrahedron Asymmetry 18 (2007) 2061–2068.
[65] J.R. Lakowicz, Principles of Fluorescence Spectroscopy, Springer, New York, 2007, pp. 55–57.
[66] V. Glushko, M. Thaler, M. Ros, The fluorescence of bilirubin upon interaction with human-erythrocyte ghosts, Biochim. Biophys. Acta 719 (1982) 65–73.
[67] V.Y. Plavskii, V.A. Mostovnikov, G.R. Mostovnikova, A.I. Tret'yakova, Spectral fluorescence and polarization characteristics of Z,Z-bilirubin IXα, J. Appl. Spectrosc. 74 (2007) 120–132.
[68] S.E. Boiadjiev, R.V. Person, D.A. Lightner, Synthesis, intramolecular hydrogen-bonding and conformation of optically active bilirubin amides — analysis by circular dichroism and NMR, Tetrahedron Asymmetry 4 (1993) 491–510.
[69] K. Maruyama, S. Awazu, H. Nishigori, M. Iwatsuru, Effects of fatty acid on the specific drug-binding sites of human serum albumin, Chem. Pharm. Bull. 34 (1986) 3394–3402.
[70] G. Bohm, R. Muhr, R. Jaenicke, Quantitative-analysis of protein far UV circular-dichroism spectra by neural networks, Protein Eng. 5 (1992) 191–195.
[71] G.V. Richieri, A.M. Kleinfeld, Unbound free fatty acid levels in human serum, J. Lipid Res. 36 (1995) 229–240.
[72] M. Pantusa, A. Stirpe, L. Sportelli, R. Bartucci, Spontaneous transfer of stearic acids between human serum albumin and PEG:2000-grafted DPPC membranes, Eur. Biophys. J. 39 (2010) 921–927.